

Cite this: *Sustainable Energy Fuels*,
2020, 4, 3143

Industrial feasibility of anodic hydrogen peroxide production through photoelectrochemical water splitting: a techno-economic analysis†

Kasper Wenderich,^a Wouter Kwak,^a Alexa Grimm,^b Gert Jan Kramer,^b
Guido Mul^a and Bastian Mei^a

Photoelectrochemical (PEC) water splitting is a promising approach to drive green, carbon-free production of hydrogen (H₂). In 'classic' water splitting, oxygen (O₂) is formed at the anode as a by-product. It has been suggested that substitution of anodic O₂ production with hydrogen peroxide (H₂O₂) could increase the financial attractiveness of PEC water splitting. Here, we present a techno-economic analysis of a photoelectrochemical H₂/H₂O₂ process. Specifically, we model photoelectrochemical farms with industrially relevant production capacities. Two scenarios are considered: (i) a theoretical scenario with an optimal solar-to-hydrogen (STH) efficiency of 27.55% and (ii) a literature-based state-of-the-art scenario with an STH efficiency of 10.1%. When applying an averaged market value of \$0.85 kg⁻¹ for H₂O₂, the analysis reveals a negative levelized cost of hydrogen (LCH) for scenario (i), *i.e.* \$6.45 kg⁻¹, and for scenario (ii) an LCH of \$6.19 kg⁻¹. Our results imply that these values are superior to the LCH of 'classic' PEC water splitting (*ca.* \$10 kg⁻¹), while the negative value for scenario (i) even outcompetes the LCH of steam methane reforming (\$1.4 kg⁻¹). We predict that significant reduction in the LCH can be realized within the PEC community when future research is aimed at enhancing the stability of the photoanode and optimizing the STH efficiency for anodic H₂O₂ formation. This manuscript clearly demonstrates the financial benefits of value-added product formation, such as hydrogen peroxide, over O₂ formation. In a broader context, our analysis verifies that further research on valuable commodity chemicals at the anode in water splitting and CO₂ reduction should be stimulated in the future to facilitate implementation of emerging, cost-intensive technologies.

Received 2nd April 2020
Accepted 17th April 2020

DOI: 10.1039/d0se00524j

rsc.li/sustainable-energy

Introduction

In the last few decades, interest in light-driven water splitting has been increasing rapidly.^{1–3} Electrochemical water splitting is foreseen to enable an environment-friendly way of harvesting and storing energy from renewable sources, such as solar energy, in the form of "green" hydrogen. In typical scenarios, hydrogen is produced in a (photo)electrochemical cell at the cathode by proton or water reduction in respectively acidic or alkaline media. Eqn (1) demonstrates the half-reaction for proton reduction:

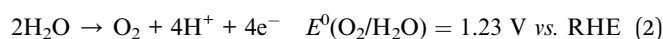


^aMESA+ Institute, Photocatalytic Synthesis Group, University of Twente, P. O. Box 217, 7500 AE Enschede, The Netherlands. E-mail: k.wenderich@utwente.nl; b.t.mei@utwente.nl; Tel: +31-53-4891985

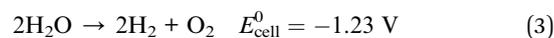
^bUtrecht University, Princetonlaan 8a, 3584 CB Utrecht, The Netherlands

† Electronic supplementary information (ESI) available: Modelling of maximum achievable STH efficiencies, flow chart demonstrating how the LCH is calculated, mathematical calculations, Matlab files used for modelling. See DOI: 10.1039/d0se00524j

Meanwhile, at the anode oxidation of water (acidic media) or hydroxide (alkaline media) takes place. The half-reaction for water oxidation is given by:



The overall reaction becomes:



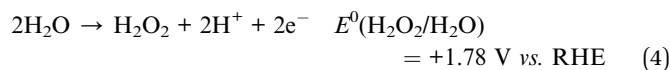
In the context of light-driven water splitting, two approaches are generally considered. In PV-E light harvesting, photovoltaic (PV) cells are coupled with water electrolysis. Generally, PV-E is considered as an appealing solution, as it allows for individual optimization of light harvesting for electricity generation and for fuel/chemical production by electrolysis. As an alternative, direct utilization of solar energy in a photoelectrochemical (PEC) cell is frequently discussed.⁴ With regard to techno-economic analyses, there is no consensus in literature whether PV-E or PEC provides the lowest average price of H₂. For example, Shaner *et al.* estimate the average levelized cost of hydrogen (LCH) to be \$12.1 kg⁻¹ and \$11.4 kg⁻¹ for base-case



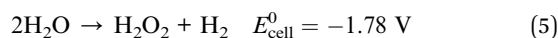
PV-E and PEC systems respectively (with plant efficiencies of *ca.* 10%),⁴ whereas more recently Grimm *et al.* predicted these prices to be \$6.22 kg⁻¹ and \$8.43 kg⁻¹ (with solar-to-hydrogen efficiencies of 10.9 and 10% respectively).⁵ Often, for PEC water splitting, the average price of H₂ is around \$10 kg⁻¹ for systems providing solar-to-hydrogen (STH) efficiencies around 10%.^{4,6,7} So far, hydrogen produced by PEC water splitting cannot compete yet with hydrogen produced by steam methane reforming (SMR), which has a current market value of \$1.4 kg⁻¹ H₂ produced.^{4,8} Development of stable, non-toxic and efficient semiconductor materials to facilitate fabrication of systems with higher STH efficiencies seems to be a straight-forward approach to invoke more industrial interest in environmental-friendly photoelectrochemical water splitting.^{9,10}

In a 'classic' (photo)electrochemical water splitting process oxygen is produced as anodic by-product (eqn (2)). With a market value of only \$35 ton⁻¹, oxygen is of low commercial interest and barely contributes to reduce the levelized cost of hydrogen (LCH).⁸ Therefore, another strategy to render PEC hydrogen production more attractive is to develop processes in which valuable products are formed at the anode.

A very alluring chemical to produce is hydrogen peroxide (H₂O₂). H₂O₂ is an important, environmental-friendly oxidant used for *e.g.* pulp and textile bleaching, disinfection, detergents, wastewater or exhaust air treatment. It is also used in chemical synthesis, semiconductor cleaning and it can be utilized in a fuel cell.^{11–15} As of 2015, 5.5 million tonnes of H₂O₂ are produced annually,¹³ mostly through the two-step anthraquinone process.^{11–18} In this process, anthraquinone is hydrogenated using *e.g.* nickel or supported palladium catalysts. The hydroquinones formed are subsequently oxidized with air, yielding H₂O₂ and regenerated anthraquinone. Afterwards, water is used for H₂O₂ extraction and distillation is applied to concentrate the H₂O₂. Despite its high usage in industry, the anthraquinone process suffers from some major drawbacks, including (but not limited to) the need for centralized production and the requirement of harmful organic solvents. A solution to these drawbacks could be the (photo)electrochemical production of hydrogen peroxide through selective two-electron oxidation of water (eqn (4)):⁸



In such case, the overall water splitting reaction becomes:



This allows for simultaneous stoichiometric production of H₂. Furthermore, such a process would allow for on-site production of H₂O₂ rather than centralized production without the need for any harmful solvents. In such a way, the need for extended transportation of a perilous substance sensitive to degradation is eliminated.^{11,12,14–19} With a current market value of \$500–1200 ton⁻¹ H₂O₂,^{8,20} hydrogen evolution with the co-production of H₂O₂ through selective water oxidation can significantly contribute to LCH reduction. This

approach can therefore be a significant economic driver for H₂-PEC development.

In 1853, Meidinger already demonstrated that hydrogen peroxide could be produced electrochemically by the electrolysis of sulfuric acid.^{11,16,21,22} Here, peroxodisulfuric acid is formed as an intermediate, which is hydrolyzed by water to eventually yield sulfuric acid and hydrogen peroxide.²³ In recent years, the interest in electrochemical H₂O₂ formation has been rekindled, where selective water oxidation has been reported both by theory and experiments.^{18,24–41} For example, MnO_x was demonstrated to work as an anode for selective water oxidation to H₂O₂.³¹ Although further material development is still required, in more recent studies metal oxides such as WO₃ and BiVO₄ seem to be excellent electrode materials, providing high selectivities for selective water oxidation to H₂O₂ at reasonable overpotentials (roughly 200 and 350 mV respectively).^{29,33} The favorable selectivity is governed by the binding energies of OH* and O* intermediates. Specifically, when ΔG_O ≥ 3.5 eV and ΔG_{OH} ≤ 2.4 eV, theory predicts that H₂O₂ should be the main water oxidation product. Pioneering work by Sayama *et al.* and Fuku *et al.*^{24–27,30} confirmed that BiVO₄ is indeed a well-suited material for the production of H₂O₂. Faradaic efficiencies (FE) of up to 80% at an applied potential of 1.5 V under simulated solar light were obtained.²⁷ Similarly, Shi *et al.* observed faradaic efficiencies ranging from *ca.* 63% up to 98% at additional potentials of 1.5 and 1.9 V *vs.* RHE respectively under (simulated) solar illumination.²⁹ Moreover, Gd:BiVO₄,³⁸ surface phosphate-treated Mo:BiVO₄,³⁹ ZnO,⁴⁰ CaSnO₃,⁴¹ germanium porphyrins⁴² and aluminum porphyrins⁴³ have been shown recently to be interesting materials for selective water oxidation to H₂O₂ as well. Lastly the inclusion of a protective layer such as mesoporous and amorphous Al₂O₃ could prevent anodic H₂O₂ degradation to O₂, thus enhancing selectivity.²⁷ For further reading, we refer the reader to one of the excellent reviews published on this topic.^{11,44,45}

Based on the presented examples it can be concluded that significant advances have been made in the development of (photo)electrochemical H₂O₂-production by selective water oxidation. Integration in PEC devices is clearly of interest. Still, the question arises whether photoelectrochemical water splitting with selective hydrogen peroxide formation is financially attractive. Along these lines, Palmer *et al.* reported that the anodic production of commodity chemicals, such as iodine and bromine, through solar approaches can financially be more rewarding than anodic oxygen evolution *via* PEC water splitting.⁴⁶ Here, we perform an in-depth techno-economic analysis of a H₂ and H₂O₂ generating PEC system that, to the best of our knowledge, is still missing. We use an optimized system, *i.e.* we consider that the required semiconductors are readily available and reactions occur with 100% faradaic efficiencies to allow for maximum solar-to-hydrogen (STH) efficiencies resembling theoretical calculations.⁸ For such systems, we calculate the levelized cost of hydrogen (LCH) for coupled H₂/H₂O₂ configurations as a function of H₂O₂ price. This system will be referred to as scenario (i). In addition, despite the novelty and therefore uncertainty, we present in scenario (ii) the techno-economics of a H₂/H₂O₂ PEC cell using recent literature data reported by Shi



et al.,²⁹ using BiVO_4 as a photoanode. To provide the required cell voltage, additional photovoltaic assistance is used. A strong dependence of LCH on the H_2O_2 price is observed. Furthermore, we predict through a sensitivity analysis that the LCH can significantly be reduced when the photoanode stability and the STH efficiency are enhanced. Importantly, for both models, we find that with reasonable H_2O_2 prices, the levelized cost of hydrogen is significantly lower in a $\text{H}_2/\text{H}_2\text{O}_2$ PEC configuration than in a H_2/O_2 PEC configuration. From a financial point of view concomitant H_2O_2 production is beneficial, and our results highlight that research to facilitate anodic H_2O_2 production should thus be stimulated.

Methodology

Overall system design

In scenario (i), we adapt the PEC module geometry of a fixed panel array reactor as described by Pinaud *et al.*⁶ and James *et al.*⁷ The fixed panel arrays are fully integrated devices and consist of two electrodes with multiple photoactive layers stacked between them. Specifically, we assume that the photoactive layer consists of two photoabsorbers with matching band gaps to allow for optimized STH efficiencies. One of the electrodes is used as a cathode for the hydrogen evolution reaction (HER), whereas the other electrode serves as an anode for the hydrogen peroxide evolution reaction (HPER). As a high pH is detrimental for the stability of H_2O_2 , we use acidic conditions in our model.^{11,16,19} A membrane is introduced between the bottom cell absorber and the anode to allow the transition of protons and separation of the cathode and anode compartments. The cathode and the anode are exposed to a continuous flow of respectively wet gas and water. A schematic depicting the fixed panel array used in our research is shown in Fig. 1. In previous

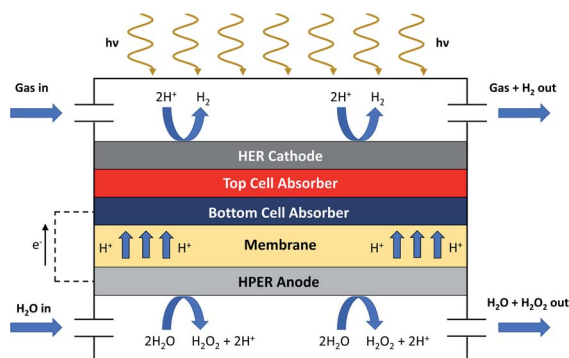


Fig. 1 Configuration of (a part of) the fixed panel array reactor used in scenario (i). Hydrogen evolution takes place at an HER cathode, whereas hydrogen peroxide evolution takes place at an HPER anode. Both electrodes are connected in series with a top cell and a bottom cell absorber, used for the absorption of solar light (depicted as wiggly arrows). A proton-exchange membrane is placed in between the bottom cell absorber and the HPER anode to allow protons to migrate from anolyte to catholyte. The top side of the reactor is made out of glass to allow light to reach the photoabsorbers. For concept clarification, a dotted line demonstrating electron movement is included in this image. It should be noted that such wiring is not physically present, as electron movement is integrated within the device itself.

work,⁸ a web-based model (WBM) developed by Seger *et al.*⁴⁷ was used to demonstrate that STH efficiencies of 27.55% can be reached when the top cell and bottom cell absorber have bandgaps of 1.9 eV and 1.2 eV respectively (in 1.0 M KOH, at 150 mV overpotential and with faradaic efficiencies of 100% for H_2 and H_2O_2 generation). Here, using the same WBM and a similar approach (with 100% faradaic efficiencies for H_2 and H_2O_2 generation), we derive that the maximum STH efficiency in 1.0 M H_2SO_4 and at 150 mV overpotential is also 27.55%, with the top and bottom cell absorbers being 1.9 and 1.2 eV as well (for additional information see ESI†).

A schematic representation of the integration of the PEC module into an industrial process is depicted in Fig. 2. The anode is constantly fed with fresh water during operation. After reaction, O_2 and a $\text{H}_2\text{O}/\text{H}_2\text{O}_2$ mixture are obtained from the water and the two products are separated. Here, the option for water evaporation to concentrate the H_2O_2 is considered as well. This is realized by distillation or rectification at moderate temperatures and low pressures.^{16,48} It should be noted that for some applications of on-site production of H_2O_2 , further concentrating of hydrogen peroxide is not needed. Here, the water is recycled afterwards. Also the electrolyte is recycled; for example, when sulfuric acid is used, steam can be used to remove water and hydrogen peroxide from the solution, similar to the Degussa–Weissenstein process.¹⁶ The resulting vapor is guided to a fractionating column, where water and hydrogen peroxide are separated. Hydrogen peroxide solution will form the output of the $\text{H}_2/\text{H}_2\text{O}_2$ PEC plant, whereas the separated water will be reused. Alternatively, calcium hydroxide can be used for the precipitation of poorly soluble calcium sulfate.⁴⁹ The precipitate is then desulfurized by thermal dissociation to form sulfur dioxide, which can be converted to sulfuric acid.⁵⁰ At the cathode, a wet gas purge is used to harvest the generated hydrogen. Consequently, the hydrogen is separated and pressurized. The wet gas is recycled as well. Separation of chemicals is assumed to occur with 100% efficiency.

Techno-economic assumptions

Similar to other reports discussing the techno-economics of PEC water splitting, a large scale facility with a daily hydrogen production of 10 tonnes is considered.^{4,6,7} A summary of the technical assumptions is shown in Table 1. Importantly, we emphasize that many of the chosen parameters are dependent

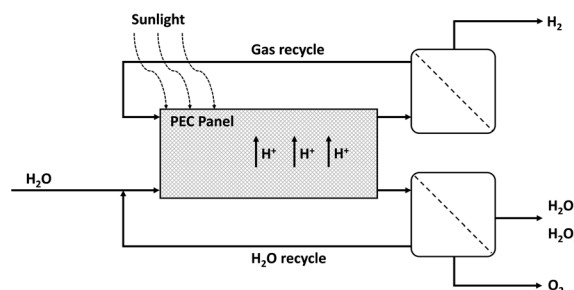


Fig. 2 Schematic of the industrial PEC process with H_2O_2 being produced at the anode and H_2 at the cathode.



Table 1 Parameter assumptions used in this work for a H₂/H₂O₂ PEC cell

Parameter	Value
H ₂ production scale ^{4,6,7}	10 t H ₂ per d
Solar energy input ^{5-7,51}	6.19 kW h m ⁻² d ⁻¹
Starting year	2020
Project lifetime ^{4,6,7}	20 years
Replacement time ^{4,5,51}	7 years
Capacity factor ^{5,51}	95%
Inflation rate ^{4,5,7,51}	1.9%
Tax rate ⁷	38.9%
Discount rate ⁷	10%
H ₂ O ₂ price range ^{8,20}	\$0.5–1.2 kg ⁻¹

on the country and precise location of the PEC plant. Here, we have chosen parameters resembling input parameters of techno-economic studies focusing on 'classic' H₂/O₂ PEC water splitting. It is assumed that the PEC panel is placed in a suitable climate for water splitting. We further explore the dependence of the levelized cost of hydrogen on such parameters in a detailed sensitivity analysis. A solar energy input of 6.19 kW h m⁻² d⁻¹ resembling the average solar energy input measured for a 35° solar panel array tilted to the south in Daggett, California, USA is used.^{5-7,51} Because the facility will face downtime due to *e.g.* defects and maintenance, we introduce a capacity factor, *i.e.* a ratio between actual operation time and theoretically possible operation time. Because most of the maintenance can be done at night, a high capacity factor of 95% is used.^{5,51} Moreover, similar to earlier reports, we adapt an inflation rate of 1.9%,^{4,5,7,51} a tax rate of 38.9%,⁷ and a discount rate of 10%.⁷ Finally, we use the known price-range of H₂O₂ in 2006, which is \$0.5–1.2 kg⁻¹.^{8,20}

For the analysis of capital expenditures (CAPEX), we distinguish between PEC cell module costs and costs related to the hard and soft balance of systems (BoS). The costs are highlighted in Table 2. Judging on previous studies,^{4,5,51} where configurations modeled for PEC water splitting to yield H₂ with O₂ as by-product are used, we estimate the base-case values of the dual photoabsorbers to be roughly \$50 m⁻². A price of \$5 m⁻², which resembles the price of a nickel-molybdenum mesh,^{5,51,52} is adopted for hydrogen evolution. The price of the anode catalyst is difficult to deduce due to the novelty of hydrogen peroxide evolution at an anode. In PEC water splitting, values of *e.g.* \$0.10 m⁻² or \$1 m⁻² have been used (for nickel),^{5,51,52} or \$8 m⁻² for the cathode and anode combined (using Pt and IrO₃).⁴ In this study, we compensate for the uncertainties associated with anodic H₂O₂ production and assume an HPER anode price of \$5 m⁻². The price of the proton-exchange membrane is set at \$50 m⁻².^{4,5,51} For the housing, a value of \$21 m⁻² is adapted.^{5,51,52} The price for glass is set at \$10 m⁻²,^{5,51,52} and the assembly costs at \$20 m⁻².^{5,51}

We determine the hard and soft balance of system (BoS) costs based on previously defined values by Grimm and co-workers.^{5,51} We adapt the same H₂ gas system of M\$11.5, which includes piping, gas compressors, condensers and intercooling. Water management is installed for a total of M\$1.3 for a PEC

Table 2 Economical costs used in this work for a H₂/H₂O₂ PEC cell

Costs	Value
CAPEX	
<i>PEC cell module</i>	
Dual photoabsorber (adapted from ref. 4, 5 and 51)	\$50 m ⁻²
HER cathode ^{5,51,52}	\$5 m ⁻²
HPER anode	\$5 m ⁻²
Membrane ^{4,5,51}	\$50 m ⁻²
Housing (adapted from ref. 5, 51 and 52)	\$21 m ⁻²
Glass ^{5,51,52}	\$10 m ⁻²
Assembly ^{5,51}	\$20 m ⁻²
<i>PEC module replacement costs</i> ^{5,51}	
	75% after 7 years & 60% after 14 years
<i>Hard BoS</i>	
H ₂ gas system ^{5,51}	M\$11.5
H ₂ O piping system (adapted from ref. 5 and 51)	M\$2.6
H ₂ O ₂ piping system	M\$2.6
Electrolyte, H ₂ O ₂ and H ₂ O separator	M\$5
Process control system	M\$6
<i>Soft BoS</i>	
Installation costs ^{5,51}	20% of initial investment + replacement costs
Contingency costs ^{5,51}	30% of initial investment
Engineering & design costs ^{5,51}	5% of initial investment
OPEX	
Insurance ^{5,7,51}	2% of initial CAPEX of PEC module and hard BoS a ⁻¹
Labor	M\$4.5 a ⁻¹

system where H₂ and O₂ are produced. We assume double costs for the piping due to double H₂O quantities required for the production of 1 mole of H₂ when H₂O₂ is produced at the anode (compare reactions (3) and (5)). Similarly, we included a H₂O₂ piping system worth M\$2.6. Due to the uncertain nature of chemical separation, an additional penalty of M\$5 was added for recycling of the electrolyte, as well as possible concentrating of the H₂O₂. Considering the process control system an expense of M\$6 was assumed that is slightly larger than that for 'normal' PEC water splitting.^{5,51} In the CAPEX costs, ground costs (\$0.15 m⁻²) are considered to be negligible.^{5,7,51}

To estimate the operating expenditures (OPEX) costs, we set an insurance of 2% of the initial capital cost.^{5,7,51} For the labor costs, we assume that 4 security officers are available all day long at any time, thus spanning 96 man-hours each day. Similarly, we assume that daily 400 man-hours are required to maintain functionality of the system, for instance realized by installing two 8 hour shifts, with 25 employees working in each shift. With an average of \$25 h⁻¹,^{5,51} the annual labor costs can be roughly estimated to be M\$4.5. Finally, the PEC cell modules will be replaced in 7 year intervals. The costs associated with panel replacement have been estimated to be 75% after 7 years and 60% after 14 years, in agreement with an expected decrease in production costs.^{5,51}



Economic model used

The net present value (NPV) of a system describes its economic profitability.^{4,51} If the $NPV < 0$, a project will have a negative profitability potential, whereas $NPV > 0$ implies that the project is economically beneficial. The break-even point of a project, where the benefits and costs outweigh each other, is defined as $NPV = 0$. Thus, in this analysis, the minimum price at which H_2 or H_2O_2 can be sold is calculated using $NPV = 0$. The NPV at the beginning of a year can be calculated using the following formula:

$$NPV = \sum_{i=0}^n \frac{CF_i}{(1+r)^i} \quad (6)$$

where CF_i is the cash flow involved in the system in the year i , r is the discount rate and n is the project lifetime in years. The cash flow is the difference between the cash flow in ($Cash_i^{in}$) and the cash flow out ($Cash_i^{out}$) minus an additional yearly tax which needs to be paid (Tax_i):

$$CF_i = Cash_i^{in} - Cash_i^{out} - Tax_i \quad (7)$$

with

$$Tax_i = (Cash_i^{in} - Cash_i^{out} - Dep_i)t_i^{rate} \quad (8)$$

Here Dep_i is depreciation (see ESI† for a detailed calculation in the corresponding M-files), which resembles the decrease in value of properties and equipment over time, whereas t_i^{rate} is the tax rate (38.9%,⁷ see Table 1). The tax only needs to be paid in years when the PEC plant makes a profit, *i.e.* when $(Cash_i^{in} - Cash_i^{out} - Dep_i) > 0$. The $Cash_i^{in}$ is defined as the income generated over the sale of the annual production of H_2 and H_2O_2 :

$$Cash_i^{in} = Income_i^{H_2} + Income_i^{H_2O_2} \quad (9)$$

or:

$$Cash_i^{in} = PX^{H_2} \times Prod_i^{H_2} + PX^{H_2O_2} \times Prod_i^{H_2O_2} \quad (10)$$

where PX is the price of H_2 or H_2O_2 and $Prod_i$ stands for the amount of H_2 or H_2O_2 produced per year. The cash outflow is dependent on the annual capital expenditures ($CAPEX_i$) and the annual operating expenditures ($OPEX_i$) (see Table 2):

$$Cash_i^{out} = CAPEX_i + OPEX_i \quad (11)$$

In our model, we use a price range of \$0.5 to 1.2 kg^{-1} for H_2O_2 (see Table 1).^{8,20} To achieve a net present value of 0, we calculate the corresponding costs at which the generated H_2 needs to be sold, *i.e.* the levelized cost of hydrogen (LCH).^{4-7,51,52} To calculate the LCH, we use a flow chart as depicted in Fig. S3.† First, the required PEC panel area is calculated using the H_2 production scale required, the faradaic efficiency towards H_2O_2 production, the solar-to-hydrogen (STH) efficiency (or simply H_2 efficiency) and several fixed parameters, *i.e.* the Gibbs free energies involved in the electrochemical production of respectively H_2O_2 and O_2 from water, the solar energy input, the capacity factor (95%, Table 1) and the molar mass of H_2 . For

a detailed derivation of the formula, we refer to the ESI (eqn (S15)†). Using the calculated PEC panel area the total OPEX and CAPEX costs and depreciation are calculated. The computed area is furthermore used to calculate the annual production of H_2O_2 (see ESI, eqn (S20)†) and thus the income over the sale of H_2O_2 . Taking into account that taxation is dependent on the CAPEX costs, the OPEX costs, the depreciation and the income over the sale of H_2O_2 and H_2 , the required income of H_2 can be calculated to achieve a net present value (NPV) of 0. From here, the minimum price at which H_2 needs to be sold is calculated in \$ per kg.

Results and discussions

Scenario (i): near optimal scenario

A contour plot of the H_2 price as a function of the solar-to-hydrogen (STH) efficiency and the H_2O_2 price is depicted in Fig. 3. A summary of the most important values derived from this figure is demonstrated in Table 3.

When the H_2O_2 price is fixed at \$0.85 kg^{-1} and an STH efficiency of 27.55% (black solid line) is assumed as predicted for an ideal PEC system (see calculations in the ESI†), the calculated H_2 price is \$6.45 kg^{-1} . Furthermore, at H_2O_2 prices of \$1.2 kg^{-1} the H_2 price is \$12.3 kg^{-1} , and even at a H_2O_2 price of \$0.5 kg^{-1} , the H_2 price is still \$0.560 kg^{-1} . Theoretically, these negative values would imply that to reach $NPV = 0$, hydrogen should be distributed while also spending additional cash. Practically, the negative values mean that there is spare room to allow for higher debits, or simply that hydrogen can be sold at a high profit. The LCH values reported here demonstrate that theoretically it is possible to photoelectrochemically produce H_2 at a cathode and H_2O_2 at an anode, and sell the H_2 at a price cheaper than \$1.4 kg^{-1} , *i.e.* the H_2 price through steam methane reforming, indicated by a red dotted line in Fig. 3. Thus, above

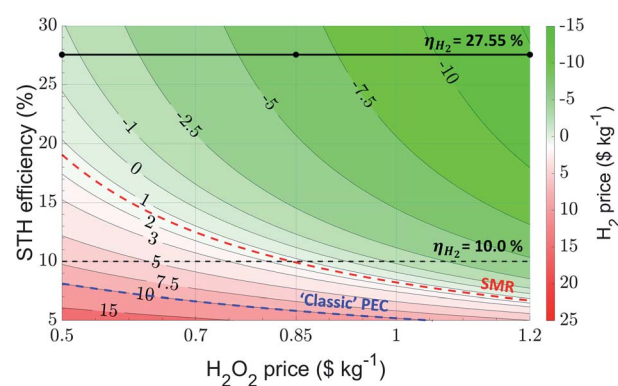


Fig. 3 Contour plot demonstrating the H_2 price as a function of the STH efficiency and H_2O_2 price using parameters defined in Tables 1 and 2 and with a faradaic efficiency of 100% for anodic H_2O_2 production. The black solid line implies the theoretical maximum of STH efficiency, the black dotted line an STH efficiency of 10%. The red dotted line corresponds to a H_2 price of \$1.4 kg^{-1} , *i.e.* the price of hydrogen formed through steam methane reforming (SMR), whereas the blue dotted line demonstrates the approximate levelized cost of hydrogen (ca. \$10 kg^{-1}) obtained using 'classic' PEC water splitting, *i.e.* through the production of O_2 at the anode.



Table 3 Important levelized cost of hydrogen (LCH) values calculated at different H₂O₂ prices and different solar-to-hydrogen (STH) efficiencies, based on parameters defined in Tables 1 and 2 and with a faradaic efficiency of 100% for anodic H₂O₂ production

H ₂ O ₂ price (\$ per kg)	STH efficiency (%)	LCH (\$ per kg)
0.5	8.11	10.0
	10.0	7.18
	19.1	1.4
	27.55	-0.560
0.85	5.82	10.0
	9.90	1.4
	10.0	1.28
	27.55	-6.45
1.2	4.54	10.0
	6.69	1.4
	10.0	-4.61
	27.55	-12.3

this line hydrogen production by PEC is favored over SMR, highlighting the general flexibility of the PEC H₂/H₂O₂ process. Using the standard case value of \$0.85 kg⁻¹ H₂O₂, a solar-to-hydrogen efficiency of only 9.90% is required to compete with SMR, whereas at respectively H₂O₂ prices of \$0.5 kg⁻¹ and \$1.2 kg⁻¹ STH efficiencies of 19.1% and 6.69% allow for competition. Although these values are relatively high, especially the values with an STH efficiency lower than 10% are not unreasonable: recent studies on photoelectrode–photovoltaic (PEC–PV) tandem cells have already demonstrated that STH efficiencies in this order of magnitude can be achieved.⁵³ Moreover, as stated above, techno-economic studies investigating ‘classic’ PEC water splitting use an STH efficiency of *ca.* 10% to achieve an LCH of *ca.* \$10 kg⁻¹.^{4,6,7} Here, our analysis of the H₂/H₂O₂ PEC system predicts H₂ prices of \$7.18 kg⁻¹, \$1.28 kg⁻¹ and \$4.61 kg⁻¹ for the H₂O₂ prices of \$0.5 kg⁻¹, \$0.85 kg⁻¹ and \$1.2 kg⁻¹ at an STH efficiency of 10% (black dotted line). In fact, to be competitive with ‘classic’ PEC water splitting (highlighted by the blue dotted line), STH efficiencies of only 8.11%, 5.82% and 4.54% are required, clearly highlighting the benefits of the H₂/H₂O₂ PEC system. In a broader view, the trends demonstrated in this section also clarify the importance of producing a valuable product at the anode: the higher the price of the product, the easier it becomes to sell H₂ at low prices.

Scenario (ii): current state-of-the-art scenario

Next, we proceed to reveal the techno-economics of a current state-of-the-art scenario, where recently published data are used as input parameters for the techno-economic model defined in this work. We use the pioneering work of Shi *et al.*,²⁹ where BiVO₄ coated on fluorine-doped tin oxide (FTO) was used as a photoanode (connected to a ‘dark’ cathode) for the production of H₂O₂ in a bicarbonate (NaHCO₃) electrolyte. Under solar simulation, the authors demonstrate that faradaic efficiencies of *ca.* 98% at current densities of 5.7 mA cm⁻² are obtained at an applied potential of 1.9 V vs. RHE. In our model, we use a hybrid PEC/PV-configuration where a photovoltaic module provides the additional voltage required to maintain the

operating potential of the system, similar to studies by Fuku *et al.*²⁶ In those studies, the required voltage was generated by double dye-sensitized solar cells (DSSCs) in combination with a BiVO₄/WO₃ photoanode. Based on previous studies,^{4,54,55} we assume that a PV cell can be optimized to yield a voltage of 1.9 V and a current of 5.7 mA cm⁻². Using the latter value, we proceed to calculate the corresponding STH efficiency using formula (S3) (defined in the ESI†). Here, it is important to note that the potential difference deviates from the commonly used 1.23 V for water splitting into hydrogen and oxygen. When oxygen is substituted with hydrogen peroxide at the anode, the thermodynamic potential becomes 1.78 V. Considering a mixed production of hydrogen peroxide and oxygen with hydrogen peroxide significantly exceeding oxygen evolution, an STH efficiency of 10.1% is calculated. To calculate the LCH, we assume a photoanode price of \$50 m⁻², which corresponds roughly to semiconductor costs used in other techno-economic analyses.^{4,5,51} We have chosen to set the price per m² of BiVO₄ high compared with the market value⁵⁶ due to uncertainties associated in the processing conditions of the photoanode. For the additional PV cell, we adapt a highly efficient multi-silicon module with a price of \$0.215 W⁻¹ and an efficiency of 18.8% as reported on EnergyTrend.⁵⁷ With a solar input of roughly 1000 W m⁻² and using the ratios between PV module cost, wiring costs and mounting costs reported earlier,⁵⁸ we estimate the total additional costs of the PV module to be \$70 m⁻². It should be noted that these costs are higher than the dual photoabsorber costs used in Table 2. This makes sense, as the dual photoabsorbers are already integrated within an operating system. Thus, no additional wiring and mounting costs are taken into account for the latter. Finally, it is important to note that in this state-of-the-art design a different electrolyte is used, rendering separation of H₂O₂ probably slightly more complex. To facilitate separation in scenario (ii) a steam process will be used as well.¹⁶ Here, sodium bicarbonate will decompose in sodium carbonate, water and carbon dioxide.⁵⁹ Thus, a vapor will be separated from the electrolyte consisting of H₂O₂, H₂O and CO₂. We propose recycling of CO₂ to maintain the ‘greenness’ of the H₂/H₂O₂ PEC process. Therefore, H₂O₂ is separated from the H₂O and the CO₂ using a fractionating column and subsequently H₂O and CO₂ are fed back to sodium carbonate solution ensuring formation of sodium bicarbonate. The resulting mixture is recycled to the PEC plant.

A schematic depicting the new configuration is demonstrated in Fig. 4. An overview of the new specifications for the techno-economic analysis is given in Table 4.

Using the new set of input parameters for scenario (ii), we calculated the levelized cost of hydrogen as a function of H₂O₂ price and STH efficiency, shown in Fig. 5. Once more, the most important values derived from this figure are summarized in Table 5.

Obviously the contour plot reveals similar trends for the LCH as the contour plot predicted for scenario (i), *i.e.* the dual photoabsorber reactor without additional voltage supply (Fig. 3). However, in contrast to the calculations shown for scenario (i), a clear offset in the contour plot for scenario (ii) is observed, *i.e.* independent of the H₂O₂ price higher STH



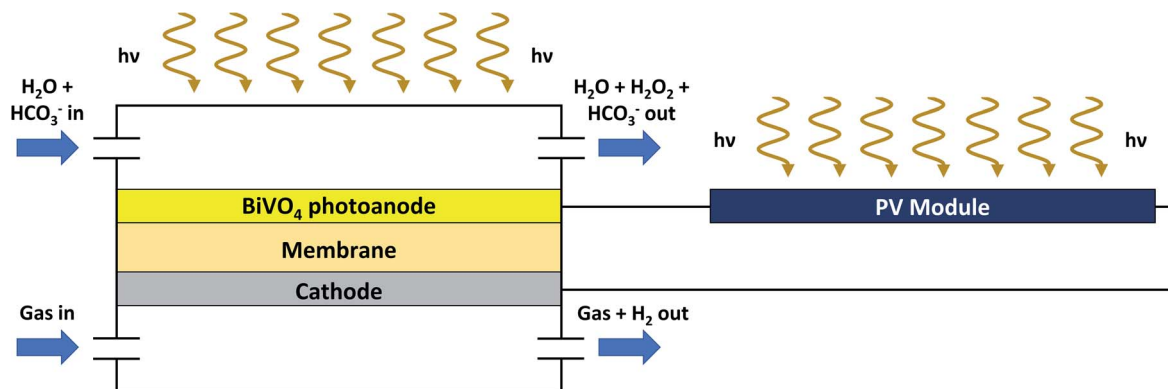


Fig. 4 Hybrid PEC/PV-configuration for the production of H_2 and H_2O_2 based on a current state-of-the-art scenario. Similar conditions as in Fig. 1 are used. In contrast, light absorption is governed both by a BiVO_4 photoanode and a photovoltaic panel. Furthermore, bicarbonate (HCO_3^-) is introduced as an electrolyte at the anodic site.

efficiencies must be achieved to allow for economically profitable H_2 production. From Fig. 5, we derive an LCH value of $\$6.19 \text{ kg}^{-1}$ when the STH efficiency is 10.1% and the hydrogen peroxide price is $\$0.85 \text{ kg}^{-1}$. Although this is not yet on par with the LCH value of H_2 produced using steam methane reforming, our analysis predicts that H_2 can be produced at lower costs than *via* 'classic' PEC water splitting. Interestingly, a slight increase in STH efficiency, *i.e.* up to 14.1%, allows for H_2 production being financially competitive with hydrogen produced through steam methane reforming (*ca.* $\$1.4 \text{ kg}^{-1}$). However, it is important to contemplate that the theoretical maximum achievable photocurrent with BiVO_4 is limited to 7.5 mA cm^{-2} .^{60,61} For anodic H_2O_2 production and cathodic H_2 production (with 100% faradaic efficiencies for both reactions) the maximum achievable STH efficiency is 13.4% (using formula (S1)[†] and a thermodynamic potential difference of 1.78 V). To achieve higher STH efficiencies (such as 14.1%), replacement of the BiVO_4 with a lower bandgap photoanode is necessary. Still, for highly efficient BiVO_4 , *i.e.* at maximum STH efficiency of 13.4%, the calculated LCH is only $\$2.06 \text{ kg}^{-1}$, nearing competition with steam methane reforming very closely.

An alternative strategy is to increase the H_2O_2 price to approximately $\$0.89 \text{ kg}^{-1}$ or $\$1.14 \text{ kg}^{-1}$ at an STH efficiency of respectively 13.4% or 10.1%. This yields an LCH competitive to steam methane reforming as well. Even further increasing the H_2O_2 price leads to even lower H_2 prices, *e.g.* $\$0.415 \text{ kg}^{-1}$ at a H_2O_2 price of $\$1.2 \text{ kg}^{-1}$. At this H_2O_2 price, an STH efficiency of 9.54% is required to compete with steam methane reforming. A low H_2O_2 price of $\$0.5 \text{ kg}^{-1}$ yields a high LCH of $\$12.0 \text{ kg}^{-1}$ (at an STH efficiency of 10.1%), which is clearly not advantageous

anymore over 'classic' PEC water splitting. Nevertheless, it is important to realize that highly optimized systems have been used to predict the LCH of 'classic' PEC water splitting, whereas here a state-of-the-art system has been considered. Still, a very high STH efficiency of 27.3% is needed to compete with steam methane reforming at such low H_2O_2 prices. Clearly, the H_2 price is very dependent on the H_2O_2 price. Therefore, it is important that H_2O_2 is sold at a sufficiently high price to make a PEC/(PV) system for H_2 and H_2O_2 production economically more attractive than SMR. Our calculations nicely reveal that a PEC/(PV) system for H_2 and H_2O_2 production can easily compete with 'classic' PEC water splitting.

Cost comparison and sensitivity analysis

As described in the methodology section, many input parameters were defined on the basis of previous techno-economic

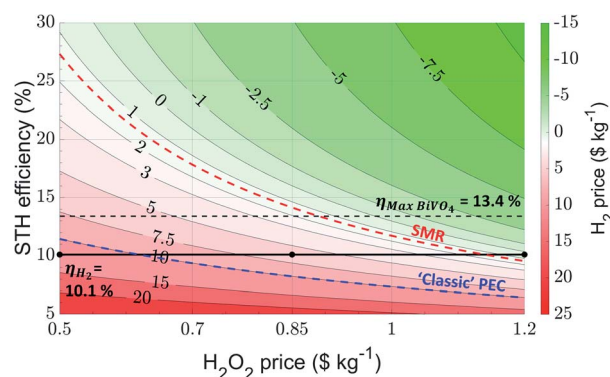


Fig. 5 Contour plot demonstrating the H_2 price as a function of the STH efficiency and H_2O_2 price based on a current state-of-the-art scenario, where a hybrid PEC/PV device configuration is used for the production of H_2 and H_2O_2 . The black line implicates the STH efficiency corresponding to the work by Shi *et al.* (10.1%).²⁹ A black dotted line is used to elucidate the theoretical maximum STH value when BiVO_4 is used as a photoanode for H_2O_2 production. The red and blue dotted lines correspond respectively to H_2 prices of $\$1.4 \text{ kg}^{-1}$ and $\$10 \text{ kg}^{-1}$. The former resembles the price of H_2 obtained through steam methane reforming (SMR), whereas the latter represents the approximate LCH obtained using 'classic' PEC water splitting.

Table 4 Alterations in the materials costs for a hybrid PEC/PV device configuration for the production of H_2 and H_2O_2 . BiVO_4 is used as a photoanode

Costs	Value
PV modules (adapted from ref. 57 and 58)	$\$70 \text{ m}^{-2}$
HPER BiVO_4 photoanode (adapted from ref. 4, 5 and 51)	$\$50 \text{ m}^{-2}$



Table 5 Important levelized cost of hydrogen (LCH) values calculated at different H_2O_2 prices and different solar-to-hydrogen (STH) efficiencies based on a current state-of-the-art scenario, where a hybrid PEC/PV device configuration is used for the production of H_2 and H_2O_2

H_2O_2 price (\$ per kg)	STH efficiency (%)	LCH (\$ per kg)
0.5	10.1	12.0
	11.4	10.0
	13.4	7.84
	27.3	1.4
0.62	10.1	10.0
	8.23	10.0
0.85	10.1	6.19
	13.4	2.06
	14.1	1.4
	13.4	1.4
1.14	10.1	10.0
	6.43	1.4
1.2	9.54	0.415
	10.1	−3.71
	13.4	−3.71

studies investigating ‘classic’ H_2/O_2 PEC water splitting. However, it is important to realize that many of these input parameters are variable and could depend on *e.g.* the country or the location where the $\text{H}_2/\text{H}_2\text{O}_2$ PEC plant is situated. Therefore, we proceed to perform a sensitivity analysis to elaborate the dependency of the LCH on various input parameters. To understand the sensitivity of our model on the predicted LCH values, we first perform a thorough analysis of the CAPEX and OPEX costs, followed by a cost variation of individual parts of the system. In Fig. 6 the magnitude of the total CAPEX and the OPEX costs during the 20 year operation of the $\text{H}_2/\text{H}_2\text{O}_2$ PEC plant for both scenario (i) and (ii) are shown. Clearly, and as expected, more expenses are involved in the current state-of-the-art scenario than in the near-optimal scenario. Especially the CAPEX costs of the PEC cell and of the soft BoS are larger, but to some extent the OPEX costs as well. The hard BoS costs remain identical. The huge increase in the CAPEX costs of the PEC cell module is due to the significant increase in materials costs: the dual photoabsorbers and the HPER anode, with a total cost of $\$55 \text{ m}^{-2}$, have been replaced by costs for both the PV modules and the BiVO_4 photoanode with a total cost of $\$120 \text{ m}^{-2}$. The dependency of the soft BoS and the OPEX costs on the PEC module costs explains the increase in those debits. It is worth noting that for the near-optimal scenario, the total CAPEX and OPEX costs are in the same order of magnitude (M\$196 *vs.* M\$150 respectively), whereas for the current state-of-the-art scenario, the CAPEX costs clearly outweigh the estimated OPEX costs (M\$626 *vs.* M\$218 respectively).

To elucidate further on the dependency of the H_2 price as a function of input parameters, we proceed by performing a sensitivity analysis for the current state-of-the-art scenario described in this work, since such a $\text{H}_2/\text{H}_2\text{O}_2$ PEC plant will be closer to implementation at this moment than one based on the near-optimal scenario. A base-case H_2O_2 price of $\$0.85 \text{ kg}^{-1}$ is used. The results of the sensitivity analysis are summarized in Fig. 7.

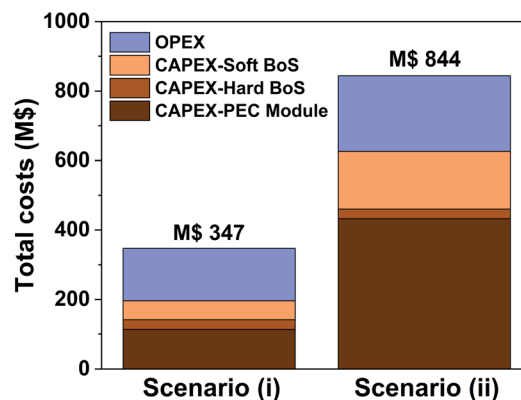


Fig. 6 Total cost comparison elucidating the magnitude of CAPEX and OPEX costs involved in cathodic H_2 production and anodic H_2O_2 production in a PEC plant producing 10 tonnes of H_2 per day. Scenario (i) demonstrates the costs for the near-optimal scenario, whereas scenario (ii) demonstrates the costs for the current state-of-the-art scenario. PV module costs are included for scenario (ii) in the PEC module CAPEX costs. The calculated area of cathodic (or anodic) material required is $3.00 \times 10^5 \text{ m}^2$ and $8.14 \times 10^5 \text{ m}^2$ for scenario (i) and (ii), respectively.

In Fig. 7a, we first highlight the difference on the influence of the CAPEX and OPEX costs on the LCH value when there is an increase of 100% or a decrease of 50%. Clearly, the influence of the CAPEX is much larger than the OPEX. This is expected, considering that the CAPEX costs make up the majority of the financial expenses for the current state-of-the-art scenario (see Fig. 6). A major change in the OPEX costs doesn't have significant implications on the LCH. Practically, this could imply that more personnel or larger wages can easily be considered to allow for a more smoothly running $\text{H}_2/\text{H}_2\text{O}_2$ PEC plant. Changes in the CAPEX costs on the other hand have quite a dramatic influence on the LCH: a reduction of 50% in the CAPEX costs reduces the LCH price from $\$6.19 \text{ kg}^{-1}$ to $\$3.19 \text{ kg}^{-1}$. On the other hand, an increase of 100% in CAPEX yields a hydrogen price of $\$25.0 \text{ kg}^{-1}$.

Clearly, the LCH sensitivity on the CAPEX is huge, and therefore we proceed to break down those CAPEX costs (Fig. 7b). To do so, the costs of the PV module and the photoanode, both large contributors in the total price, and the replacement time of the PEC module are evaluated. For the PV module, we assumed a total cost of $\$70 \text{ m}^{-2}$, where mounting materials and wiring costs are included.^{57,58} However, Shaner *et al.* adopt a much larger total PV price of $\$141 \text{ m}^{-2}$,⁴ which would yield a H_2 price of $\$11.5 \text{ kg}^{-1}$ in our study. For the photovoltaic module costs, the authors adopt prices for non-subsidized, single crystalline Si PV modules from the year 2015, whereas we adopt prices of a highly efficient multi-silicon module in 2019 from the same database (*i.e.* EnergyTrend).⁵⁷ Clearly, prices of PV modules are dropping. Therefore, it is also realistic to assume that in the future, the prices might even be lower. If the price of the PV module is halved, the LCH is only $\$3.60 \text{ kg}^{-1}$, a considerable improvement compared to the LCH of $\$6.19 \text{ kg}^{-1}$ predicted for the base-case of scenario (ii). As expected, sensitivity analysis for the photoanode costs shows similar



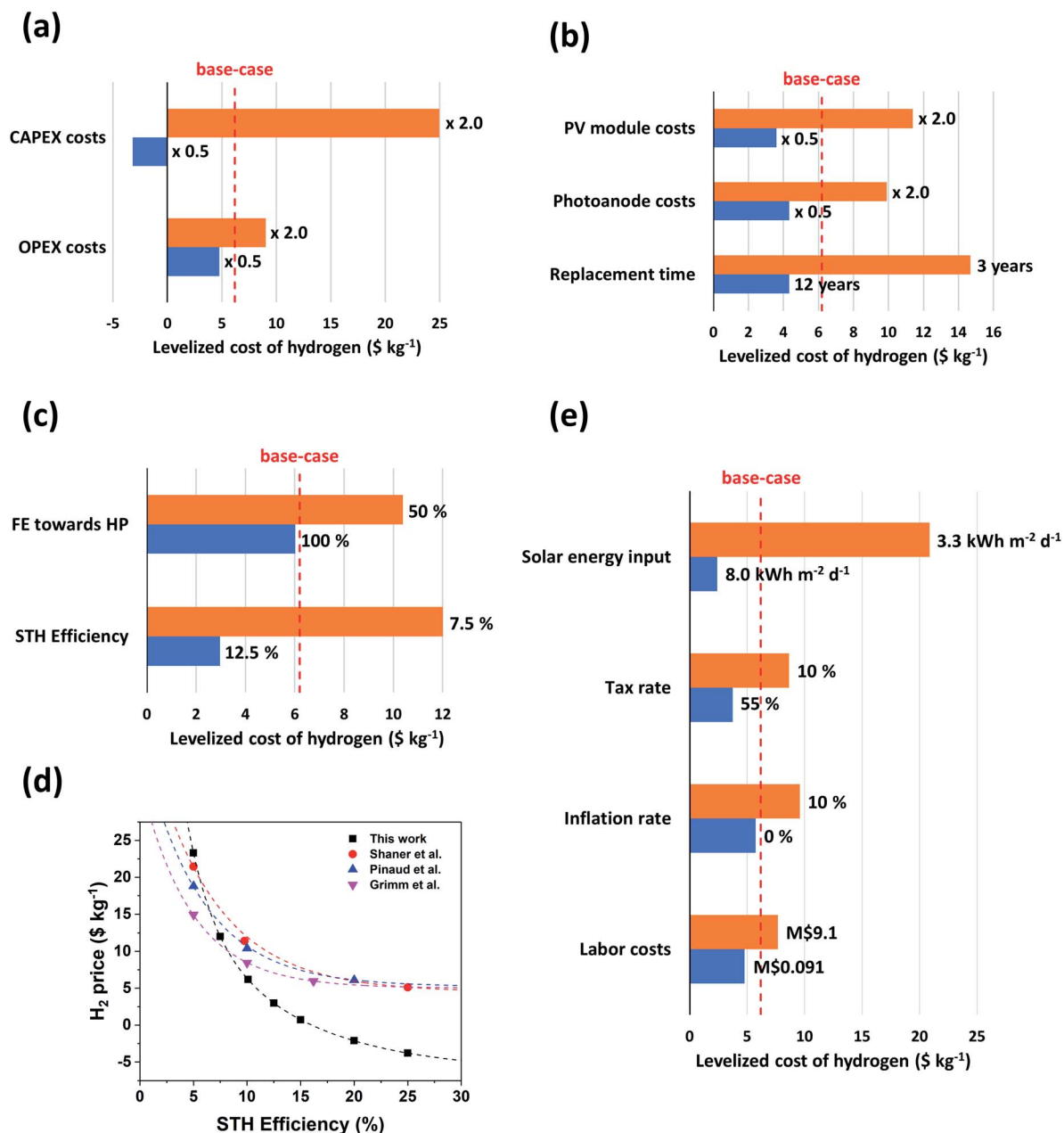


Fig. 7 Sensitivity analysis for the current state-of-the-art scenario of a H₂/H₂O₂ PEC plant. The LCH is plotted as a function of (a) CAPEX and OPEX costs; (b) PV module costs, photoanode costs and replacement time; (c) faradaic efficiency towards hydrogen peroxide (HP) production and STH efficiency and (e) solar energy input, tax rate, inflation rate and labor costs. The red dotted line indicates the base-case LCH value, *i.e.* \$6.19 kg⁻¹ H₂ at a H₂O₂ price of \$0.85 kg⁻¹, a faradaic efficiency of 98% an STH efficiency of 10.1% and a replacement time of 7 years. The base-case values of (e) are defined in Tables 1 and 2. (d) Comparison of the LCH as a function of STH efficiencies in this work and other works from literature.^{4–6}

trends as for the PV module costs. In this work, we estimate the cost to be \$50 m⁻².^{4,5,51} However, because of the novelty of anodic hydrogen peroxide production, little is known yet about the material best suited for anodic H₂O₂ production. Correspondingly the materials price is hard to estimate. If the photoanode cost is doubled, an LCH of \$9.90 kg⁻¹ is calculated. However, a reduction of the cost is rewarding: half the price of the photoanode cost would yield an LCH of \$4.34 kg⁻¹. The price range for the PV module and photoanode indicates that

industrial development of large scale H₂/H₂O₂ PEC systems can be attainable in the near future. Another important feature is the durability of the PEC module. In fact, if the PEC module has to be replaced frequently, the consequences for the LCH are significant. When the PEC module is replaced already after every 3 years, the hydrogen price more than doubles (\$14.7 kg⁻¹). When replacement is done every 12 years (practically meaning that replacement is done only once in the 20 years of operation), the LCH would be \$4.33 kg⁻¹. Clearly, material



stability is one of the most important factors that needs to be considered for a profitable $\text{H}_2/\text{H}_2\text{O}_2$ PEC plant. Therefore improvement of the durability of the HPER electrode should be stimulated.

Moreover, we study the influence of the faradaic efficiency (FE) to H_2O_2 production and the solar-to-hydrogen (STH) efficiency of the system (Fig. 7c). As indicated in eqn (S3),[†] the STH efficiency is amongst others dependent on the FE towards H_2O_2 . In the current state-of-the-art scenario, the FE for H_2O_2 was almost 100%. Care should be taken to have sufficient FE; reduction of the FE to 50% for instance would imply an increase of the LCH to $\$10.4 \text{ kg}^{-1}$. In fact, a faradaic efficiency of 0% to H_2O_2 production would mean a faradaic efficiency of 100% to O_2 production. Thus, the PEC system becomes a 'classic' PEC water splitting system. In such a case, the LCH would be $\$14.8 \text{ kg}^{-1}$. This value is slightly higher than LCH values for a 'classic' H_2/O_2 PEC system reported in literature at an STH efficiency of 10% (ca. $\$10 \text{ kg}^{-1}$).^{4,6,7}

The influence of the STH efficiency on the LCH is much larger in our model. An increase of the STH efficiency from 10.1% to 12.5% yields an astonishing LCH drop to $\$2.97 \text{ kg}^{-1}$. Similarly, a decrease in STH efficiency to 7.5% yields an LCH value of $\$12.0 \text{ kg}^{-1}$. In previous studies on the technoeconomics of 'classic' PEC water splitting, the high dependency of the hydrogen price on STH efficiency has also been reported.⁴⁻⁶ In Fig. 7d, we compare the dependency of the H_2 price as a function of the STH efficiency in our work with the values reported in those studies. Clearly, we predict that this dependency is more extreme for a $\text{H}_2/\text{H}_2\text{O}_2$ PEC system than for a H_2/O_2 PEC system. This also means that an identical change in STH efficiency is more rewarding for the $\text{H}_2/\text{H}_2\text{O}_2$ PEC system. At STH efficiencies higher than 8.3%, the $\text{H}_2/\text{H}_2\text{O}_2$ PEC system yields lower LCH values than the best performing H_2/O_2 PEC system reported by Grimm *et al.*⁵ Thus, selective water oxidation to H_2O_2 over O_2 is more rewarding at those STH efficiencies. Clearly, controlling the STH efficiency is a crucial factor in achieving profitable $\text{H}_2/\text{H}_2\text{O}_2$ PEC plants. As the FE towards H_2O_2 is already close to 100%, other aspects need to be improved to attain higher STH efficiencies. The only non-fixed variable which allows for this is the operating current density (see eqn (S3)[†]). Hence, researchers should look for ways to increase the current density while maintaining similar faradaic efficiencies, e.g. by optimizing the BiVO_4 photoanode or development of highly efficient anodes with smaller bandgap, similar to the materials development strategies used for 'classic' PEC water splitting devices.

Finally, we investigate the dependency of the LCH on parameters influenced by the location and country of the $\text{H}_2/\text{H}_2\text{O}_2$ PEC plant, specifically the solar energy input, the tax rate, the inflation rate and the labor costs. The results are summarized in Fig. 7e. For the solar energy input, we base a negative scenario on the solar energy input in Enschede, The Netherlands; for a positive scenario the Atacama Desert in northern Chile was chosen. With optimal tilt of the panels, the solar energy inputs are respectively $3.3 \text{ kW h m}^{-2} \text{ d}^{-1}$ and ca. $8.0 \text{ kW h m}^{-2} \text{ d}^{-1}$.⁶² These inputs yield LCH values of respectively $\$20.9 \text{ kg}^{-1}$ and $\$2.40 \text{ kg}^{-1}$, revealing the significant dependence

of the LCH on the location of the $\text{H}_2/\text{H}_2\text{O}_2$ PEC plant. Thus, it is vital to locate the plant in a dry and sunny area, such as California, the Atacama Desert, Australia, the Arabian Desert or the Sahara Desert in Africa. This is of course also true for 'classic' PEC water splitting devices. The influence of the tax rate is considerably less: an increase in tax rate to 55% (possible in the United Arab Emirates) yields an LCH of $\$8.66 \text{ kg}^{-1}$, whereas using a tax rate of 10% (used in e.g. Qatar) results in an LCH of $\$3.76 \text{ kg}^{-1}$.⁶³ Similarly, the influence of the inflation rate is also not high. Increasing the inflation to a high value of 10% would yield a hydrogen price of $\$9.59 \text{ kg}^{-1}$, whereas no inflation would imply a hydrogen price of $\$5.76 \text{ kg}^{-1}$. Finally, we proceed to break down labor costs. Based on averaged incomes, we roughly estimate that a high salary for employment in the $\text{H}_2/\text{H}_2\text{O}_2$ PEC plant could be $\$50 \text{ h}^{-1}$ and a low salary could be $\$0.50 \text{ h}^{-1}$ (for instance possible when the plant would be located in Switzerland or Ethiopia, respectively).⁶⁴ This would correspond roughly with annual labor costs of $\text{M}\$9.1 \text{ a}^{-1}$ and $\text{M}\$0.091 \text{ a}^{-1}$. Implementation in our sensitivity analysis yields values of $\$7.68 \text{ kg}^{-1} \text{ H}_2$ and $\$4.76 \text{ kg}^{-1} \text{ H}_2$, rendering the consequence of labor costs for the predicted H_2 price small. This result is in line with the prediction that the sensitivity of the LCH on the OPEX costs is significantly lower than the sensitivity of the LCH on the CAPEX costs.

Concluding, our sensitivity analysis of the current state-of-the-art scenario predicts that the design and implementation of a $\text{H}_2/\text{H}_2\text{O}_2$ PEC system approaches financial feasibility. For the base-case scenario, the LCH is already advantageous over a 'classic' PEC water splitting system. Even when a negative scenario for a variable is assumed (with the exception of the total CAPEX costs and the solar energy input), the LCH value is close to or is even still lower than the H_2 price predicted for 'classic' PEC water splitting devices. Similarly, when an optimistic scenario is assumed, possible competition of a $\text{H}_2/\text{H}_2\text{O}_2$ PEC system with steam methane reforming draws nearer. Specifically, judging by the strong dependency of the LCH, an increase in the STH efficiency seems critical. Materials stability also seems a key factor: while an increase in lifetime only yields a limited reduction of the H_2 price, a decrease has detrimental effects. Finally, by far the most defining parameter for the choice of location and country would be the solar energy input. It is recommended to install the PEC plant in a sun-drenched environment.

Discussion

In this work, we clearly demonstrated the high potential of reducing the hydrogen price by selective photoelectrochemical water splitting with hydrogen peroxide production at the anode. In fact, when the market value of H_2O_2 and the STH efficiency is sufficiently high, a $\text{H}_2/\text{H}_2\text{O}_2$ PEC configuration will be competitive with hydrogen production obtained through steam methane reforming. In this manuscript, we assumed a H_2O_2 price range of $\$0.5 \text{ kg}^{-1}$ to $\$1.2 \text{ kg}^{-1}$. However, the data used to estimate the H_2O_2 price are from 2006, and thus the H_2O_2 market value is expected to be higher in the current year 2020. Indeed, the price of 50% H_2O_2 on Kemcore is $\$0.75 \text{ kg}^{-1}$.⁶⁵ In



such case, the price for pure 100% H_2O_2 would be $\$1.5 \text{ kg}^{-1}$. Fig. 3 and 5 clearly demonstrate that a higher H_2O_2 price is advantageous for achieving a lower H_2 price. To be competitive with hydrogen produced from steam methane reforming, this would also mean that a lower solar-to-hydrogen efficiency is needed. Thus, it would be easier to actually achieve this competitiveness.

In the sensitivity analysis we predicted that a $\text{H}_2/\text{H}_2\text{O}_2$ PEC system is close to financial feasibility. We have demonstrated that, aside from the location of the $\text{H}_2/\text{H}_2\text{O}_2$ PEC plant, especially the improvement of the STH efficiency is important to achieve competitiveness with steam methane reforming. Furthermore, it is important that stable materials are used. Research on anodic materials for hydrogen peroxide production is still very novel. Consequently, there is plenty of opportunity to improve materials on solar-to-hydrogen and solar-to-hydrogen peroxide efficiencies, as well as on stability. In our model, for the state-of-the-art scenario, we assumed that BiVO_4 is stable. However, later studies by Baek *et al.* have demonstrated that the stability of BiVO_4 during H_2O_2 production is insufficient.³⁸ Strategies to overcome this could be the addition of a protective layer (*e.g.* Jeon *et al.* use phosphate treatment on $\text{Mo}:\text{BiVO}_4$),³⁹ or to dope the material with a stabilizing agent (Baek *et al.* use gadolinium (Gd) for instance).³⁸ Still, we chose to use BiVO_4 as a model in this study, as we believe that stable anodes with a similar price range and with similar photoelectrochemical properties can be engineered in the future. Alternatively, rather than employing a photoelectrochemical cell for hydrogen and hydrogen peroxide production, a photovoltaic-electrolytic system can be used. Here, an optimized anode for the production of hydrogen peroxide needs to be found.

An important feature of $\text{H}_2/\text{H}_2\text{O}_2$ PEC systems on the industrial scale is that hydrogen peroxide can be produced on-site, as opposed to the anthraquinone process.^{11,12,14,15,17,18} This is a big advantage, considering that hydrogen peroxide is a hazardous chemical and is very prone to decomposition when trace amounts of catalyst (such as metal ions) are present.^{16,19} Prolonged transport of hydrogen peroxide with the addition of a stabilizer is thus not required anymore. Still, it is good to keep in mind that even with on-site production, conditions for the fast decomposition of H_2O_2 should be avoided. H_2O_2 is significantly unstable in basic conditions, particularly when the pH is larger than 9.^{11,19} Qiang *et al.* also reported some degree of H_2O_2 decomposition around a pH-value of 3, possibly due to the trace presence of ferrous iron. Therefore, we advise to perform H_2O_2 generation in (preferably strong) acidic conditions. Here, in scenario (ii), we made use of a bicarbonate (HCO_3^-)-containing solution. Typically, bicarbonate acts as a buffer through an equilibrium with carbonic acid ($\text{CO}_2 + \text{H}_2\text{O}$, $\text{p}K_a = 6.4$) and carbonate (CO_3^{2-} , $\text{p}K_a = 10.3$).^{24,66,67} A fresh bicarbonate solution without any pH adjustment will have a pH around 8. This would be in the 'safe' pH-range of H_2O_2 stability. Still, lowering of the pH through CO_2 purging could be considered. Alternatively, the bicarbonate could be substituted with an electrolyte with strong acidic properties. For instance, judging by its usage in history for H_2O_2 production, sulfuric acid could be a potential candidate.^{11,16,21–23} Furthermore, it is also important that the

H_2O_2 is not exposed to temperatures higher than room temperature to prevent decomposition.¹⁹ Therefore, cooling down of the H_2O_2 after synthesis might be rewarding as well.

In the production of an industrial $\text{H}_2/\text{H}_2\text{O}_2$ PEC system, it is very important that the energy required to build the plant does not exceed the chemical energy harvested. In literature, this concept is referred to as the renewable energy factor (REF),^{68,69} or the energy return on energy invested (EROEI).^{70,71} The EROEI can be calculated using the following formula:

$$\text{EROEI} = \frac{T \times E_H}{E_P + (T \times E_O) + E_D} \quad (12)$$

where T is the lifetime of the plant in years, E_H is the yearly chemical energy stored in hydrogen, E_P is the energy used for the production of the plant, E_O is the yearly energy used for facility operation and E_D is the energy used when the facility is decommissioned. It is important that the EROEI (or REF) exceeds a value of 1: a smaller value implies that more (brown) energy is required to build and maintain the plant than that the plant produces green energy, *i.e.* the $\text{H}_2/\text{H}_2\text{O}_2$ PEC plant would not be renewable anymore. Evidently, the lifetime and chemical energy stored should be maximized, whereas the sum of the energy for plant production, operation and decommissioning should be minimized. Sathre *et al.*^{70,71} have thoroughly investigated the life-cycle net energy assessment of a 'classic' H_2/O_2 PEC water splitting plant. They concluded that the most important factors contributing to the EROEI are (in decreasing order of relevance): (1) the STH efficiency, (2) the cell life span and (3) the energy intensity of cell fabrication. To obtain an EROEI above 1, the authors recommend in their latest study to employ STH efficiencies considerably larger than 5%, having cell life spans exceeding 5 years and using low-energy thin film deposition processes. Moreover, the location of the PEC plant is also advocated to be important by the authors. There are remarkable parallels between the works of Sathre *et al.*^{70,71} and our own: once more, the importance for scientists to work on the STH efficiency and the stability is highlighted, and the location of the PEC plant should not be neglected.

To increase the EROEI value (and thus the 'greenness' of the $\text{H}_2/\text{H}_2\text{O}_2$ PEC plant) even further to well above 1, a strategy would be to concentrate solar energy on the PEC module (and, if used, the additional PV module). A tracking concentrator array could be used to achieve such light concentration.^{4,6,7} Typically, a parabolic cylinder array is used to focus solar light on a (linear) PEC module and a tracking system is used to align the concentrator array for optimal solar illumination harvesting during the day. Such devices can concentrate solar illumination to a factor of 10. As demonstrated in the sensitivity analysis in Fig. 7e, increasing the light intensity per m^2 would also result in a steep decrease of the LCH. Larger concentration factors are possible, but care should be taken that currents larger than 1 A cm^{-2} are avoided. This is due to catalyst limitations, bubble formation (which scatter light) and temperature constraints.^{6,72}

In a broader context, we have demonstrated in this study that (photo)electrochemical hydrogen evolution becomes more interesting when a valuable product at the anode is formed. Although sustainable H_2 production at the TW level can only be



achieved through water splitting, co-(photo)electrolysis might facilitate market penetration of the required PEC systems. Particularly, we have demonstrated that scenario (ii) already nears competition with steam methane reforming. Besides H_2O_2 , chlorine gas (Cl_2), bromine gas (Br_2) and sodium hydroxide (NaOH) are usually advocated as interesting anodic products.^{8,54} More recently, Palmer *et al.* showed that also fluorine, iodine, methane decomposition (to carbon), potassium permanganate, sodium bromate, sodium chlorate and sodium persulfate production should be considered.⁴⁶ They based this on the calculation of the net value of the chemicals per unit of energy input. Although in this study a black box approach has been used without taking CAPEX and OPEX costs into account, it still gives a good overview on which commodity chemicals might be interesting to be produced by means of a photoelectrochemical system. It should be mentioned that the study of Palmer *et al.* also demonstrates that substitutes for hydrogen at the cathode, for example tellurium, cobalt or tungsten, could be interesting to synthesize through (photo) electrochemical means while producing hydrogen peroxide at the anode. Alternatively, the (photo)electrochemical reduction of carbon dioxide with concomitant hydrogen peroxide should be considered too.⁷³ Moreover, it was also recently demonstrated that hydrogen peroxide could be produced at both the anode and the cathode from selective water oxidation and oxygen reduction respectively.^{26,28,39}

When we use the method of Palmer *et al.* to calculate the net value per unit of energy input for H_2O_2 (with hydrogen at the cathode),⁴⁶ we find a value of $\$0.30 \text{ kW h}^{-1}$ when the H_2O_2 price is $\$0.85 \text{ kg}^{-1}$. In comparison, the anodic synthesis of bromine, iodine and sodium bromate, as well as the anodic decomposition of methane to carbon, yield a higher maximum net value per energy and are thermodynamically more favorable. Therefore, they could be worthwhile of investigation as well. Still, the market size of hydrogen peroxide is larger than for those chemicals (with the exception of methane decomposition to carbon),^{13,46} implying that hydrogen production with concomitant hydrogen peroxide production is still one of the most rewarding approaches to achieve industrial implementation of PEC water splitting.

Conclusions

In this work, we performed a techno-economic analysis to investigate the feasibility of anodic hydrogen peroxide production as a substitute for oxygen to decrease the levelized cost of hydrogen (LCH) in photoelectrochemical (PEC) water splitting. Using a near-optimal scenario, only an STH efficiency of 9.90% is needed to compete with steam methane reforming at a H_2O_2 price of $\$0.85 \text{ kg}^{-1}$. For a current state-of-the-art scenario with an STH efficiency of 10.1% and also a H_2O_2 price of $\$0.85 \text{ kg}^{-1}$, an LCH of $\$6.19 \text{ kg}^{-1}$ was calculated, an obvious improvement compared to LCH values found in 'classic' water splitting. Clearly, this study demonstrates the financial advantages of replacing oxygen at the anode in PEC water splitting with hydrogen peroxide. Therefore, further research of photoelectrochemical H_2O_2 production at the anode should be

stimulated. A sensitivity analysis on the current state-of-the-art scenario demonstrates that reduction of the CAPEX costs will contribute to allow $\text{H}_2/\text{H}_2\text{O}_2$ PEC systems (here connected to additional photovoltaic modules) to be financially competitive with hydrogen formation through steam methane reforming. Key factors in reducing this cost will be the improvement of the STH efficiency, optimization of stability and choosing a sunlit location for the $\text{H}_2/\text{H}_2\text{O}_2$ PEC plant. Research on novel materials for hydrogen peroxide production should be stimulated, while simultaneously the importance of the stability should not be neglected. Once the anode material has been properly engineered, anodic H_2O_2 production could have a promising future in industry for hydrogen production through (photo-) electrochemical means. In a broader context, we have demonstrated that the production of a valuable commodity chemical at an anode could play a key role for obtaining LCH's in PEC water splitting competitive with the LCH's in steam methane reforming.

Conflicts of interest

There are no conflicts to declare.

Abbreviations

BoS	Balance of systems
CAPEX	Capital expenditures
DSSCs	Dye-sensitized solar cells
EROEI	Energy return on energy invested
FE	Faradaic efficiency
FTO	Fluorine-doped tin oxide
HER	Hydrogen evolution reaction
HP	Hydrogen peroxide
HPER	Hydrogen peroxide evolution reaction
LCH	Levelized cost of hydrogen
NPV	Net present value
OPEX	Operating expenditures
PEC	Photoelectrochemical
PV	Photovoltaic(s)
PV-E	Photovoltaic-electrolysis
REF	Renewable energy factor
SMR	Steam methane reforming
STH efficiency	Solar-to-hydrogen efficiency
STHP efficiency	Solar-to-hydrogen peroxide efficiency
WBM	Web-based model

Acknowledgements

The authors are grateful to Mats Wildlock and Nina Simic from Nouryon (Bohus, Sweden) for fruitful discussions. Also, we would like to thank the Topconsortium voor Kennis- en Innovatie Biobased Economy (TKI-BBE) (TKI-BBE 1803), the Topconsortium voor Kennis- en Innovatie Chemie (TKI Chemie) (Chemie.PGT.2019.007) and Nouryon for financial support. Alexa Grimm is acknowledging financial support by Shell Global Solutions.



References

- 1 T. Hisatomi, J. Kubota and K. Domen, *Chem. Soc. Rev.*, 2014, **43**, 7520–7535.
- 2 A. Kudo and Y. Miseki, *Chem. Soc. Rev.*, 2009, **38**, 253–278.
- 3 F. E. Osterloh, *Chem. Soc. Rev.*, 2013, **42**, 2294–2320.
- 4 M. R. Shaner, H. A. Atwater, N. S. Lewis and E. W. McFarland, *Energy Environ. Sci.*, 2016, **9**, 2354–2371.
- 5 A. Grimm, W. A. De Jong and G. J. Kramer, *Int. J. Hydrogen Energy*, 2020, submitted.
- 6 B. A. Pinaud, J. D. Benck, L. C. Seitz, A. J. Forman, Z. Chen, T. G. Deutsch, B. D. James, K. N. Baum, G. N. Baum, S. Ardo, H. Wang, E. Miller and T. F. Jaramillo, *Energy Environ. Sci.*, 2013, **6**, 1983–2002.
- 7 B. D. James, G. N. Baum, J. Perez and K. N. Baum, *Technoeconomic analysis of photoelectrochemical (PEC) hydrogen production*, Directed Technologies Inc., Arlington, Virginia, 2009.
- 8 B. Mei, G. Mul and B. Seger, *Adv. Sustainable Syst.*, 2017, **1**, 1600035.
- 9 J. Joy, J. Mathew and S. C. George, *Int. J. Hydrogen Energy*, 2018, **43**, 4804–4817.
- 10 J. Chen, D. Yang, D. Song, J. Jiang, A. Ma, M. Z. Hu and C. Ni, *J. Power Sources*, 2015, **280**, 649–666.
- 11 S. Yang, A. Verdaguier-Casadevall, L. Arnarson, L. Silvioli, V. Čolić, R. Frydendal, J. Rossmeisl, I. Chorkendorff and I. E. L. Stephens, *ACS Catal.*, 2018, **8**, 4064–4081.
- 12 J. M. Campos-Martin, G. Blanco-Brieva and J. L. G. Fierro, *Angew. Chem., Int. Ed.*, 2006, **45**, 6962–6984.
- 13 R. Ciriminna, L. Albanese, F. Meneguzzo and M. Pagliaro, *ChemSusChem*, 2016, **9**, 3374–3381.
- 14 Y. Jiang, P. Ni, C. Chen, Y. Lu, P. Yang, B. Kong, A. Fisher and X. Wang, *Adv. Energy Mater.*, 2018, **8**, 1801909.
- 15 S. Fukuzumi, Y. Yamada and K. D. Karlin, *Electrochim. Acta*, 2012, **82**, 493–511.
- 16 G. Goor, J. Glenneberg, S. Jacobi, J. Dadabhoy and E. Candido, in *Ullmann's Encyclopedia of Industrial Chemistry*, Wiley-VCH Verlag GmbH & Co. KGaA, Weinheim, Germany, 2019, pp. 1–40.
- 17 C. Samanta, *Appl. Catal., A*, 2008, **350**, 133–149.
- 18 K. Sayama, *ACS Energy Lett.*, 2018, **3**, 1093–1101.
- 19 Z. Qiang, J.-H. Chang and C.-P. Huang, *Water Res.*, 2002, **36**, 85–94.
- 20 ICIS, www.icis.com/chemicals, accessed Jan 2017.
- 21 S. Ranganathan and V. Sieber, *Catalysts*, 2018, **8**, 379.
- 22 H. Meidinger, *Liebigs Ann.*, 1853, **88**, 57–81.
- 23 H. Berthelot, *C. R. Acad. Sci.*, 1878, **86**, 71–76.
- 24 K. Fuku and K. Sayama, *Chem. Commun.*, 2016, **52**, 5406–5409.
- 25 K. Fuku, Y. Miyase, Y. Miseki, T. Gunji and K. Sayama, *ChemistrySelect*, 2016, **1**, 5721–5726.
- 26 K. Fuku, Y. Miyase, Y. Miseki, T. Funaki, T. Gunji and K. Sayama, *Chem.-Asian J.*, 2017, **12**, 1111–1119.
- 27 K. Fuku, Y. Miyase, Y. Miseki, T. Gunji and K. Sayama, *RSC Adv.*, 2017, **7**, 47619–47623.
- 28 X. Shi, Y. Zhang, S. Siahrostami and X. Zheng, *Adv. Energy Mater.*, 2018, **8**, 1801158.
- 29 X. Shi, S. Siahrostami, G.-L. Li, Y. Zhang, P. Chakthranont, F. Studt, T. F. Jaramillo, X. Zheng and J. K. Nørskov, *Nat. Commun.*, 2017, **8**, 701.
- 30 Y. Miyase, S. Takasugi, S. Iguchi, Y. Miseki, T. Gunji, K. Sasaki, E. Fujita and K. Sayama, *Sustainable Energy Fuels*, 2018, **2**, 1621–1629.
- 31 A. Izgorodin, E. Izgorodina and D. R. MacFarlane, *Energy Environ. Sci.*, 2012, **5**, 9496–9501.
- 32 C. McDonnell-Worth and D. R. MacFarlane, *RSC Adv.*, 2014, **4**, 30551–30557.
- 33 S. Siahrostami, G.-L. Li, V. Viswanathan and J. K. Nørskov, *J. Phys. Chem. Lett.*, 2017, **8**, 1157–1160.
- 34 V. Viswanathan, H. A. Hansen and J. K. Nørskov, *J. Phys. Chem. Lett.*, 2015, **6**, 4224–4228.
- 35 Y. Ando and T. Tanaka, *Int. J. Hydrogen Energy*, 2004, **29**, 1349–1354.
- 36 A. Naldoni, T. Montini, F. Malara, M. M. Mróz, A. Beltram, T. Virgili, C. L. Boldrini, M. Marelli, I. Romero-Ocaña, J. J. Delgado, V. Dal Santo and P. Fornasiero, *ACS Catal.*, 2017, **7**, 1270–1278.
- 37 Z. Han, K. T. Horak, H. B. Lee and T. Agapie, *J. Am. Chem. Soc.*, 2017, **139**, 9108–9111.
- 38 J. H. Baek, T. M. Gill, H. Abroshan, S. Park, X. Shi, J. Nørskov, H. S. Jung, S. Siahrostami and X. Zheng, *ACS Energy Lett.*, 2019, **4**, 720–728.
- 39 T. Jeon, H. Kim, H.-i. Kim and W. Choi, *Energy Environ. Sci.*, 2020, DOI: 10.1039/c9ee03154e.
- 40 S. R. Kelly, X. Shi, S. Back, L. Vallez, S. Y. Park, S. Siahrostami, X. Zheng and J. K. Nørskov, *ACS Catal.*, 2019, **9**, 4593–4599.
- 41 S. Y. Park, H. Abroshan, X. Shi, H. S. Jung, S. Siahrostami and X. Zheng, *ACS Energy Lett.*, 2019, **4**, 352–357.
- 42 T. Shiragami, H. Nakamura, J. Matsumoto, M. Yasuda, Y. Suzuri, H. Tachibana and H. Inoue, *J. Photochem. Photobiol., A*, 2015, **313**, 131–136.
- 43 F. Kuttassery, S. Mathew, S. Sagawa, S. N. Remello, A. Thomas, D. Yamamoto, S. Onuki, Y. Nabetani, H. Tachibana and H. Inoue, *ChemSusChem*, 2017, **10**, 1909–1915.
- 44 S. Fukuzumi, Y.-M. Lee and W. Nam, *Chem.-Eur. J.*, 2018, **24**, 5016–5031.
- 45 J. Liu, Y. Zou, B. Jin, K. Zhang and J. H. Park, *ACS Energy Lett.*, 2019, **4**, 3018–3027.
- 46 C. Palmer, F. Saadi and E. W. McFarland, *ACS Sustainable Chem. Eng.*, 2018, **6**, 7003–7009.
- 47 B. Seger, O. Hansen and P. C. K. Vesborg, *Sol. RRL*, 2017, **1**, e201600013.
- 48 K. V. Titova, V. P. Nikol'skaya, V. V. Buyanov and I. P. Suprun, *Russ. J. Appl. Chem.*, 2002, **75**, 1903–1906.
- 49 A. E. Simpson and C. A. Buckley, *Desalination*, 1988, **70**, 431–442.
- 50 J. M. Stinson and C. E. Mumma, *Ind. Eng. Chem.*, 1954, **46**, 453–457.
- 51 W. A. De Jong, Master thesis, Utrecht University, 2018.
- 52 M. Victoria, PhD thesis, Delft University of Technology, 2015.



- 53 J. H. Kim, D. Hansora, P. Sharma, J.-W. Jang and J. S. Lee, *Chem. Soc. Rev.*, 2019, **48**, 1908–1971.
- 54 E. Chinello, M. A. Modestino, J. W. Schüttauf, L. Coulot, M. Ackermann, F. Gerlich, A. Faes, D. Psaltis and C. Moser, *RSC Adv.*, 2019, **9**, 14432–14442.
- 55 S. Tembhrune and S. Haussener, *Sustainable Energy Fuels*, 2019, **3**, 1297–1306.
- 56 *Kremer Pigmente; Bismuth-Vanadate Yellow, lemon*, <https://www.kremer-pigmente.com/en/1422/bismuth-vanadate-yellow-lemon>, accessed Mar 2020.
- 57 EnergyTrend, <https://www.energytrend.com/solar-price.html>, accessed Nov 2019.
- 58 *International Technology Roadmap for Photovoltaic (ITRPV) - Results 2018 including maturity report 2019*, October 2019.
- 59 C. Thieme, in *Ullmann's Encyclopedia of Industrial Chemistry*, Wiley-VCH Verlag GmbH & Co. KGaA, Weinheim, Germany, 2019, pp. 299–317.
- 60 F. F. Abdi, N. Furet and R. van de Krol, *ChemCatChem*, 2013, **5**, 490–496.
- 61 P. Luan and J. Zhang, *ChemElectroChem*, 2019, **6**, 3227–3243.
- 62 *Global Solar Atlas*, <https://globalsolaratlas.info/map>, accessed Mar 2020.
- 63 D. Bunn, *Tax Foundation: Corporate Tax Rates Around the World*, 2018, <https://taxfoundation.org/corporate-tax-rates-around-world-2018>, accessed Mar 2020.
- 64 *WorldData.info: average income around the world*, <https://www.worlddata.info/average-income.php>, accessed Mar 2020.
- 65 Kemcore, <https://www.kemcore.com/hydrogen-peroxide-50.html>, accessed Feb 2020.
- 66 G. Czapski, S. V. Lymar and H. A. Schwarz, *J. Phys. Chem. A*, 1999, **103**, 3447–3450.
- 67 W. W. Rudolph, G. Irmer and E. Königsberger, *Dalton Trans.*, 2008, 900–908.
- 68 F. Kuttassery, S. Mathew, S. N. Remello, A. Thomas, K. Sano, Y. Ohsaki, Y. Nabetani, H. Tachibana and H. Inoue, *Coord. Chem. Rev.*, 2018, **377**, 64–72.
- 69 F. Kuttassery, D. Yamamoto, S. Mathew, S. N. Remello, A. Thomas, Y. Nabetani, A. Iwase, A. Kudo, H. Tachibana and H. Inoue, *J. Photochem. Photobiol., A*, 2018, **358**, 386–394.
- 70 R. Sathre, C. D. Scown, W. R. Morrow, J. C. Stevens, I. D. Sharp, J. W. Ager, K. Walczak, F. A. Houle and J. B. Greenblatt, *Energy Environ. Sci.*, 2014, **7**, 3264–3278.
- 71 R. Sathre, J. B. Greenblatt, K. Walczak, I. D. Sharp, J. C. Stevens, J. W. Ager and F. A. Houle, *Energy Environ. Sci.*, 2016, **9**, 803–819.
- 72 O. Khaselev and J. A. Turner, *Science*, 1998, **280**, 425–427.
- 73 M. Jouny, W. Luc and F. Jiao, *Ind. Eng. Chem. Res.*, 2018, **57**, 2165–2177.

